Eva Rajo-Iglesias
Departamento de Teoria de la Señal y Comunicaciones
University Carlos III of Madrid
Despacho 4.3B10
Avenida de la Universidad,
30, 28911 Leganés, Madrid, Spain
Tel: +34 91 624 8774;
Fax: +34 91 624 8749
E-mail: eva@tsc.uc3m.es

Printed Multi-Band MIMO Antenna Systems and Their Performance Metrics

Mohammad S. Sharawi

Electrical Engineering Department
King Fahd University of Petroleum and Minerals (KFUPM)
Dhahran, 31261 Saudi Arabia
Tel: + (966) 3860-4810; Fax: + (966) 3860-3535; E-mail: msharawi@kfupm.edu.sa

Abstract

Multiple-input-multiple-output (MIMO) antenna systems are a key enabling technology for modern fourth-generation (4G) wireless systems. The need for higher data rates for multimedia applications within the limited bandwidth and power levels led the way to the use of multiple antennas at the receiver and transmitter ends. Printed MIMO antenna systems, supporting multiple bands, including the lower band of the 4G wireless standard (LTE), pose a challenge in terms of available size. In this work, we start by defining the new required metrics to characterize MIMO antenna systems. We then present several recent printed multi-band MIMO antenna systems, along with some isolation-enhancement mechanisms that are used in these closely packed antennas.

Keywords: Printed antennas; multiple-input-multiple-output (MIMO); correlation coefficient; total active reflection coefficient (TARC); mean effective gain (MEG); branch power ratio; mutli-band

1. Introduction

Multiple-input-multiple-output (MIMO) antenna systems are currently used in almost all 4G wireless terminals. The use of multiple antennas increases the data rate within the limited bandwidth and power levels. In an ideal situation, the channel capacity obtained is directly proportional to the number of transmitter and receiver antennas within a multipath environment, according to [1]

$$C = B\log_2\left(1 + M \times N \times SNR\right), \quad (1)$$

where C is the channel capacity in bits/sec, B is the channel bandwidth in Hz, and M and N are the number of transmitter antennas and receiver antennas, respectively. SNR is the signal-to-noise ratio (absolute value). To be able to embed and integrate multiple antennas at the user terminal, size becomes a major limiting factor. In addition, to have useful antenna operation, the antennas need to cover multiple bands of opera-

tion. This poses another challenge for the antenna designer. The need for compact MIMO antennas with good performance metrics is thus a major task for wireless-terminal designers.

It is well known that antenna miniaturization will affect the performance of the antenna, especially its efficiency and operating bandwidth [2]. In addition, the placement of multiple antennas in very close vicinity, such as in a mobile phone, will increase the antenna coupling between the closely radiated fields, as well as the shared ground (GND) plane. This will affect the diversity performance of the MIMO antenna system [3]. A compromise among antenna size and performance metrics has to be identified, and all parameters should be optimized for the best performance, given the design-size constraints.

Several printed MIMO antenna systems have appeared in the literature in the past few years, targeting the fourth generation of wireless devices, and covering a wide range of frequencies. Figure 1 shows the growing number of published papers in this area since 2009. It is just a representation of the growing number, and is based on extensive searches within the databases of the IEEE (IEEE Xplore) and Wiley (*Microwaves and Optical Technology Letters – MOTL*). The numbers are based on collecting only printed MIMO antenna papers from more than 450 papers located with the keyword "MIMO" in IEEE Xplore, and collecting all the printed MIMO antenna papers that came from the Wiley *MOTL* database in a similar way. The number of papers published under this category (printed MIMO antennas) in the year 2012 exceeded 55, which is a clear indication of the importance of and the practical interest in this technology.

Another interesting trend from the past few years is the increased focus on multi-band MIMO antenna systems that can provide backward compatibility with existing 2G and 3G wireless systems, as well as covering the 4G standards, along with WLAN, among others. Looking closer into the numbers from Figure 1, Figure 2 shows the number of multi-band printed-MIMO-antenna published works since the year 2009. When talking about multi-band, most of the work presented in the literature focused on the higher bands of the various wireless standards, as designing for multi-band operation with one of the bands covering GSM 800 MHz, for example, is very challenging. This is because in the lower bands, the coupling between the adjacent antennas that are so close to one another (within a 50 mm × 100 mm surface area) becomes large, thus degrading the diversity performance of the printed MIMO antenna system. Figure 3 shows the number of papers that appeared in literature that covered a band that was lower than 1 GHz within its multi-band operation. The numbers were very few compared to Figure 2, meaning that this is an area of great interest, due to its practical benefits in real wireless devices.

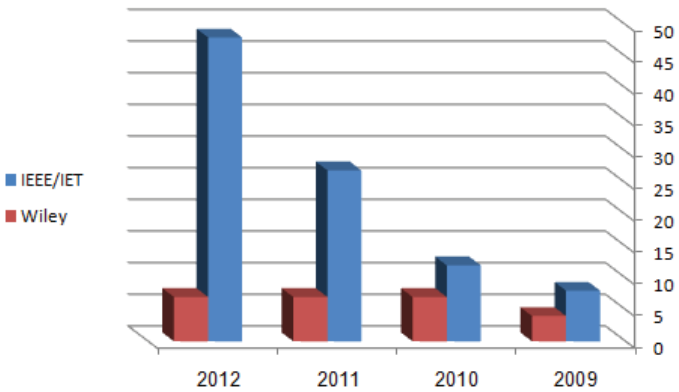

Figure 1. The number of published works in the area of printed MIMO antenna systems between 2009-2012.

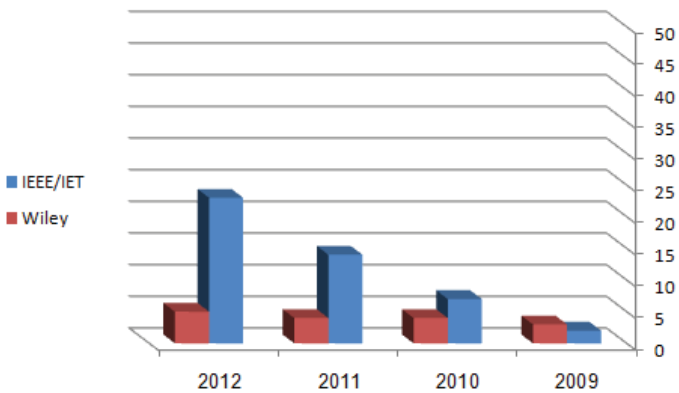

Figure 2. The published printed multi-band MIMO antenna systems between 2009-2012.

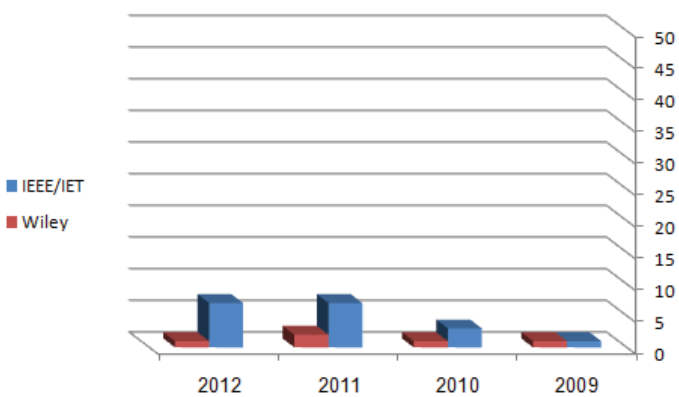

Figure 3. The published printed multi-band MIMO antenna systems with one of the bands covering lower than 1 GHz between 2009-2012.

In this article, we will briefly go over the performance metrics that are required to characterize the behavior of MIMO antennas. We then will present some of the latest printed multiband antennas that have recently appeared in the literature, along with their isolation-enhancement mechanisms and their performance metrics.

2. Performance Metrics for MIMO Antenna Systems

Along with the conventional antenna-performance metrics and parameters, such as the bandwidth, the resonance frequency, the radiation patterns, the gain, and the efficiency, several important parameters need to be evaluated to fully characterize a MIMO antenna system. These metrics are not essential in single-antenna devices, but they are essential for multi-antenna devices. These performance metrics are discussed in the following subsections.

2.1 The Correlation Coefficient

The correlation coefficient (ρ) is a measure that describes how much the communication channels are isolated or correlated with each other. This metric considers the radiation pattern of the antenna system, and how much the patterns affect one another when operated simultaneously (which is the case in a MIMO antenna system). The square of the correlation coefficient is known as the envelop correlation coefficient. The envelop correlation coefficient (ρ_e) can be calculated using the following formula [4]:

$$\rho_e = \frac{\left|\iint_{4\pi}\left[\vec{F}_1(\theta,\varphi) * \vec{F}_2(\theta,\varphi)\right] d\Omega\right|^2}{\iint_{4\pi}\left|\vec{F}_1(\theta,\varphi)\right|^2 d\Omega \iint_{4\pi}\left|\vec{F}_2(\theta,\varphi)\right|^2 d\Omega}, \quad (2)$$

where $\vec{F}_i(\theta,\varphi)$ is the three-dimensional field radiation pattern of the antenna when the *i*th port is excited, and Ω is the solid angle. The asterisk is the Hermitian product operator. This is a complicated expression that requires three-dimensional radiation-pattern measurements and numerical integration. Equation (2) is valid when a uniform multipath environment of balanced polarization is considered (i.e., an isotropic environment). A simple derivation in [4] showed that the correlation coefficient can be calculated using the *S* parameters when a lossless and single-mode antenna is considered. The effect of the efficiency on the envelope-correlation-coefficient calculation from the *S* parameters was added in [5]. This expression is given by

$$\left|\rho_{ij}\right|^2 = \rho_{eij} = \left| \frac{\left|S_{ii}^* S_{ij} + S_{ji}^* S_{jj}\right|}{\sqrt{\left(1-\left|S_{ii}\right|^2-\left|S_{ji}\right|^2\right)\left(1-\left|S_{jj}\right|^2-\left|S_{ij}\right|^2\right)\eta_{radi}\eta_{radj}}} \right|^2, \quad (3)$$

where ρ_{ij} is the correlation coefficient between elements *i* and *j*, ρ_{eij} is the envelop correlation coefficient, S_{ij} is the *S* parameter between the *i*th and *j*th elements (coupling), and η_{radi}, η_{radj} are the radiation efficiencies of elements *i* and *j*, respectively. In this formula, we need to know only the *S* parameters and the radiation efficiencies, which can be easily evaluated, as compared to the three-dimensional radiation patterns required by Equation (2). A correlation coefficient value of 0.3 has been set as an acceptable value for 4G wireless systems [6].

The terms coupling and isolation are usually interchanged in the literature as low coupling yields high isolation. More specifically, isolation is usually found directly from the *S* parameters ($\text{isolation} = -10\log_{10}\left(\left|S_{ij}\right|\right)$). It is important to mention that the isolation and correlation coefficient are two different quantities. Although Equation (3) shows that lower coupling (high isolation) yields lower correlation, it only accounts for isolation between the input ports of the antennas through the antenna's structure, and does not account for radiated field coupling, while Equation (2) does. Low coupling (high isolation) thus does not guarantee a low correlation coefficient, and vice versa. High isolation and low correlation coefficients are required for a MIMO antenna system to provide good diversity performance.

Low correlation between channel multipath streams (and thus antenna element fields) can be achieved when each individual multipath incoming wave is given a specific weight at each antenna element, based on its angle of arrival (AoA). This can be achieved via spatial diversity (antenna locations), angle diversity (antenna-pattern magnitude and phase response), or polarization diversity (the polarization behavior of the antennas with respect to one another) [7]. Some examples employing such techniques were presented in [8, 9]. It has to be emphasized that low correlation is a necessary but not sufficient condition for good MIMO performance, as the channel has to have some certain characteristics, as well.

2.2 Total Active Reflection Coefficient (TARC)

To properly characterize the efficiency and bandwidth (BW) of the MIMO antenna system, the scattering matrix is not enough [10]. For better characterization of the MIMO antenna system, the total active reflection coefficient (TARC) is used. The TARC is defined as the ratio of the square root of the total reflected power divided by the square root of the total incident power [11] in a multi-port antenna system. The TARC can be computed using the *S* parameters of the MIMO antenna system. For an *N*-element antenna, the TARC is given by

$$\Gamma_a^t = \frac{\sqrt{\sum_{i=1}^{N} |b_i|^2}}{\sqrt{\sum_{i=1}^{N} |a_i|^2}} \qquad (4)$$

where a_i and b_i are the incident signals and reflected signals, respectively. These can be computed from the measured *S* parameters. The relationship between the incident and reflected waves in a multi-port network with similar characteristic impedances at all ports is given by [12]

$$\mathbf{b} = \mathbf{S}\mathbf{a}, \qquad (5)$$

where **S** is the *S*-parameter matrix. The bold face in Equation (5) indicates a vector quantity with magnitude and phase. For an *N*-port MIMO antenna system, the *S*-parameter matrix will thus become $N \times N$. The TARC accounts for coupling as well as random-signal combinations between ports. The TARC has a value between zero and one, where zero means all power was radiated, while one means all incident power was reflected and nothing was radiated. The available power is the sum of powers available on all the ports of the antenna system. The TARC is usually presented in decibels.

The TARC also includes the effect of a feeding phase to the antenna port. A single curve of the TARC can hence be used to determine the resonance frequency and impedance bandwidth of the whole antenna system for a specified phase excitation between the ports [13]. For a two-port MIMO antenna system, the TARC (Γ_a^t) can be evaluated using [14]:

$$\Gamma_a^t = \frac{\sqrt{\left(\left|S_{11} + S_{12}e^{j\theta}\right|^2\right) + \left(\left|S_{21} + S_{22}e^{j\theta}\right|^2\right)}}{\sqrt{2}}, \qquad (6)$$

where θ is the input feeding phase, S_{xx} is the reflection coefficient of the port, and S_{xy} is the coupling between the two ports associated with the antenna structure. Once the *S* parameters of a two-port network are found, the random phase is swept between 0° and 180° to investigate the effect of the phase variation between the two ports on the resonance behavior of the antenna, and to thus create the corresponding TARC curves for effective bandwidth assessment.

If the TARC for a multi-port antenna system is needed for more than two ports, Equation (5) is used in conjunction with Equation (4). Port 1 is excited with a signal having unity amplitude and zero phase (i.e., $1e^{j0}$), while the other ports are excited with similar amplitudes but different phases. After applying Equation (5) to get the reflected signal values (b_i) from the incident (excitation) values (a_i), Equation (4) is then used to find the TARC values.

2.3 Mean Effective Gain (MEG)

The standalone antenna gain (i.e., the gain calculated for single antenna elements) is not a good measure of antenna performance, as the antenna is not used in an anechoic chamber, in practical applications. The antenna is used in a certain environment for a specific application. The study of the effect of the environment on the antenna's radiation characteristics is thus important in evaluating its true performance. One way to do this is to fabricate an antenna, operate it under the specific conditions along with another standard antenna with known characteristics, and get the antenna's performance. We have to fabricate a prototype, test it to get the results, tune the antenna, and repeat the process to get the desired design. This procedure is very time consuming and costly. The practical method of calculating mean effective gain was described in [15].

A solution to this problem was proposed in [16], where a probabilistic model for the environment was proposed. Using the three-dimensional radiation patterns along with the proposed statistical model, one can get mean effective gain numerically by solving a mathematical expression that combines the two quantities. This numerical method allows us to get mean effective gain using the simulated/measured gain patterns in an ideal environment (i.e., the simulation tool or an anechoic chamber), and a model of the environment suitable for the application for which the antenna is being designed. The mathematical expressions for the mean effective gain calculation are shown in Equations (7) and (8):

$$MEG = \int_0^{2\pi}\int_0^{\pi}\left[\frac{XPD}{1+XPD}G_\theta(\theta,\varphi)P_\theta(\theta,\varphi) + \frac{1}{1+XPD}G_\varphi(\theta,\varphi)P_\varphi(\theta,\varphi)\right]\sin\theta d\theta d\varphi \qquad (7)$$

The following conditions must be satisfied:

$$\int_0^{2\pi}\int_0^{\pi}\left[G_\theta(\theta,\varphi)+G_\varphi(\theta,\varphi)\right]\sin\theta d\theta d\varphi = 4\pi\,, \qquad (8a)$$

$$\int_0^{2\pi}\int_0^{\pi} P_\theta(\theta,\varphi)\sin\theta d\theta d\varphi = \int_0^{2\pi}\int_0^{\pi} P_\varphi(\theta,\varphi)\sin\theta d\theta d\varphi = 1 \qquad (8b)$$

$$XPD = \frac{P_V}{P_H} \qquad (9)$$

where XPD is the cross-polarization power ratio (or cross-polarization discrimination), which represents the distribution of the incoming power (the ratio between the vertical mean incident power to the horizontal mean incident power), $G_\theta(\theta,\phi)$ and $G_\phi(\theta,\phi)$ are antenna gain components, and $P_\theta(\theta,\phi)$ and $P_\phi(\theta,\phi)$ represent the statistical distribution of the incoming waves in the environment, assuming that the two are not correlated. The equations in Equation (8) represent the conditions needed for evaluating Equation (7). A more general formulation using the polarization matrix and other incoming wave distributions can be found in [17, 18].

There are a number of channel models available in the literature. A channel model suits a particular environment, such as urban, rural, etc. A general channel model was given in [16]. This model assumed a uniform distribution for the signals in the azimuth direction, and a Gaussian distribution in the elevation direction. This represented a regular Rayleigh fading channel for cellular communications. This model required three-dimensional radiation-pattern measurement and processing. To simplify the process, the incoming waves were assumed to be concentrated only in the horizontal plane. This assumption significantly reduces the complexity of mean effective gain calculation [19].

2.4. Diversity Gain (DG)

Diversity is usually achieved when the transmitter receives multiple versions of the transmitted stream through different channel paths (since we have multiple antennas). If the signals are uncorrelated, the combined signals at the receiver will provide higher signal-to-noise-ratio levels, and thus better signal reception. Diversity gain is a measure of the effect of diversity on the communication system. Diversity gain (more specifically, the effective diversity gain) is defined as the difference between the time-averaged SNR of the combined signals within the diversity antenna system and that of a single antenna system in one diversity channel, provided the SNR is above a reference level. Mathematically, the diversity gain is defined as follows [20]:

$$Diversity\ \ Gain = \left[\frac{\gamma_c}{SNR_c} - \frac{\gamma_1}{SNR_1}\right]_{P(\gamma_c<\gamma_s/SNR)}, \qquad (10)$$

where γ_c and SNR_c are the instantaneous and mean SNR for the diversity system, respectively, and γ_1 and SNR_1 are the instantaneous and mean SNR for the single branch with maximum values in the diversity system. γ_s/SNR is the reference level. Assuming uncorrelated signals with a Rayleigh distribution, the probability that the instantaneous mean SNR of the diversity system is less than the reference level [$P(\gamma_c<\gamma_s/SNR)$] can be approximated as

$$P\left(\gamma_c<\frac{\gamma_s}{SNR}\right) = \left[1-e^{\left(-\frac{\gamma_s}{SNR}\right)}\right]^M, \qquad (11)$$

where M is the number of antennas. The increase in the number of antennas will increase the received combined power in a diversity system (MIMO system). Figure 4 shows the effective diversity gain obtained as a function of the number of antenna branches according to Equation (11), when maximum-ratio combining is used (the branches with higher SNR get more weight and are used in the receiver). The 1% point on the curves corresponds to 99% reliability, and is the mark where diversity gain is accessed. As can be seen, the more antenna elements, the larger the obtained gain, up until six or higher, where the amount of gain obtained offers little to the gain improvement. The diversity gain and correlation coefficient are related. The lower the correlation coefficient, the higher is the diversity gain.

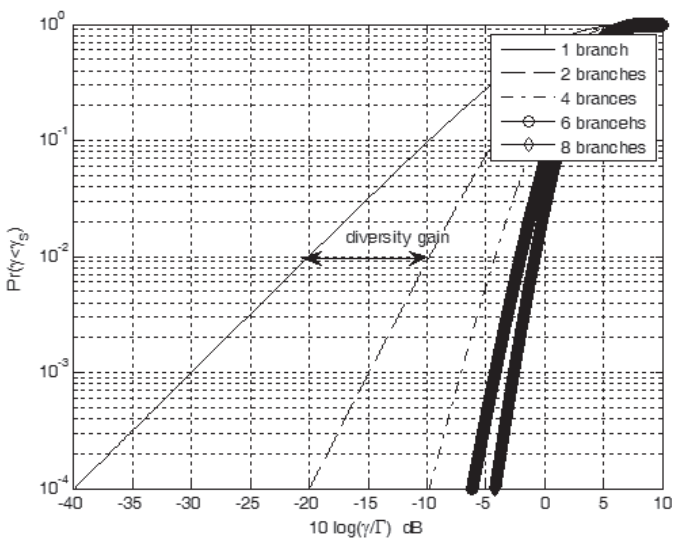

Figure 4. The cumulative distribution function of Equation (11), showing the diversity gain obtained as a function of the increase in the number of antenna elements.

2.5 Branch Power Ratio

Other factors that affect the performance of a MIMO antenna system are the relative power levels coming from the different antenna branches. The power levels of the various branches should be very close. To represent these power-level differences, we introduce the two-branch power-level ratio (k) as

$$k = \frac{P_{min}}{P_{max}}, \tag{12}$$

where P_{min} is the power level of the antenna with the lower power, and P_{max} is the power from the higher-power antenna. The power-level ratio will affect the diversity gain, as the overall obtained diversity gain is multiplied with the inverse of k to obtain the actual effective diversity gain. This causes Equation (11) to become

$$P\left(\gamma_c < \frac{\gamma_s}{SNR}\right) \approx \frac{1}{k}\left[1 - e^{\left(-\frac{\gamma_s}{SNR}\right)}\right]^M. \tag{13}$$

The branch-power ratio (k) can also be found from the mean effective gain values calculated from a MIMO antenna system. For a two-element MIMO antenna system [3],

$$k = \min\left(\frac{MEG_2}{MEG_1}, \frac{MEG_1}{MEG_2}\right), \tag{14}$$

where MEG_1 and MEG_2 are the mean effective gains of antennas 1 and 2, respectively. To obtain the maximum diversity gain and avoid significant loss in the diversity performance of the MIMO antenna system, k should be more than -3 dB (between 0 dB to -3 dB).

2.6 System Capacity

The main advantage of a MIMO antenna system is that it provides an improved channel capacity in a multipath environment as compared to a single-input-single-output (SISO) system. The upper bound of the channel capacity of a MIMO antenna system is therefore also a performance metric. The channel capacity of a MIMO antenna system depends on the channel matrix, which is a function of the radiation characteristics of the antenna elements and the channel environment. In case of an N-element MIMO antenna, when the channel conditions are not known to the transmitter, equal power is allocated to each element of the MIMO antenna system at the transmitter side. The channel capacity in bits/sec/Hz under these circumstances is given as

$$C = \log_2\left[\det\left(I_N + \frac{\rho}{N}HH^T\right)\right], \tag{15}$$

where ρ is the average SNR, H is the normalized channel covariance matrix, I_N is an $N \times N$ identity matrix, and N is the number of antenna elements at the receiver as well as at the transmitter side.

In the case of uncorrelated transmitting/incoming waves, antenna elements with zero correlation coefficients at both the transmitter and the receiver – with similar powers and normalized mean effective gain values – yield an identity matrix for HH^T, and a linear increase in channel capacity is obtained as compared to a SISO system when the number of antenna elements increases. Equation (15) thus becomes

$$C = N \times \log_2\left(1 + \frac{\rho}{N}\right). \tag{16}$$

This is an ideal channel-capacity limit of a MIMO system. This limit cannot be achieved, since there is always some correlation between the channels, and the correlation coefficient between the antenna elements is never zero. The higher mutual coupling between the antenna elements and the higher correlation in the channel thus results in more degradation in the performance of a MIMO antenna system. It is important to note that in a line-of-sight (LOS) environment, when all the channels are totally correlated, the performance of a MIMO antenna is nothing but that of a SISO antenna with an increase in the effective aperture of the antenna due to multiple elements. The real use of MIMO antenna systems is thus in multipath environments, which exist in practical wireless mobile communication applications. In such environments, the H matrix contains the information of the correlation between different channels due to antenna, as well as due to the propagation environment. The calculation of the channel-coefficient matrix, H, of a MIMO antenna system operating in a particular environment is thus important, as it relates the channel capacity of the antenna in that environment. Different channel-modeling methods employed to find the channel-coefficient matrix have been investigated in the literature for the multipath environment, such as that in [21].

3. Printed Multi-Band MIMO Antennas

Several printed multi-band MIMO antenna systems have appeared in the literature, such as those in [22-41]. The majority of printed multi-band MIMO antennas that have appeared in the literature cover frequency bands higher than 1 GHz. This will provide the system with better isolation, due to the increase in the spatial separation in terms of wavelengths at higher bands of operation. Multi-band antennas with one band covering less than 1 GHz are few in the literature, due to the challenge of maintaining high isolation and a low correlation coefficient. In this section, we will present several printed multi-band antennas that have appeared in the literature, along with their performance metrics and design tradeoffs. The section is divided into two parts. One part presents examples of multi-band printed MIMO antennas covering higher than 1 GHz bands. The other part considers those covering lower than 1 GHz bands (at least one of the multi-bands covered).

3.1 Multi-Band Printed MIMO Antenna Systems with Higher than 1 GHz Operation

The list of examples in this category is large, and this can be seen from Figure 2. Usually, these multi-band printed MIMO antenna systems cover frequencies that are higher than 2 GHz, with a few covering higher than 1 GHz. Some few recent works in this area include [22-32]. Due to the high frequency of operation, high isolation levels are achieved for these antenna types. In addition, spatial separation (between the two edges of a mobile handset) can significantly improve the isolation, due to the shorter wavelength of operation. Some isolation techniques will be presented for some of the antennas in this category, when we discuss their performance. The examples chosen are such that they cover different antenna types for different applications.

In [23], a dual-element dual-band MIMO antenna system operating at WLAN 2.4 GHz and 5.8 GHz bands was proposed. The antenna consisted of two printed back-to-back monopole elements, with an isolation stub for isolation improvement. The measured isolations were 25 dB and 20 dB at the 2.45 GHz and 5.8 GHz bands, respectively. The isolation enhancement using the shorted stub was 15 dB and 5 dB in the lower and higher bands, respectively. The two antennas were connected via a microstrip line that had a perpendicular stub shorted to the ground plane. The stub had two lengths from its connection point with the connecting line: one controlled the isolation level at the lower band (the one shorted to ground), and the other controlled the higher-band isolation level. This isolation structure reduced the ground surface currents near element 2 when element 1 was excited by trapping the currents within it, thus enhancing the isolation.

The correlation coefficient obtained was lower than 0.1 for this printed MIMO antenna system. The total size of the antennas without the ground plane was 15 mm × 50 mm × 0.8 mm. Figure 5a shows the fabricated prototype, and Figure 5b shows the measured *S* parameters. The maximum measured gain values were 4.12 dBi at 2.45 GHz and 4.86 dBi at 5.75 GHz. The efficiency, the TARC, and the mean effective gain were not specified.

A dual-broadband dual-element printed MIMO antenna system covering 1.5 GHz to 2.8 GHz as the first broad band and 4.7 GHz to 8.5 GHz as the second broad band was proposed in [29]. The MIMO antenna system consisted of two concentric open rectangular loops. Figure 6a shows the fabricated antenna structure. The antennas occupied 63 mm × 50 mm × 0.8 mm of substrate size. An FR-4 material with dielectric constant of 4.4 was used. Figure 6b shows the measured *S* parameters of the proposed antenna. Note that a decoupling U-shaped slot in the ground (a defected ground) was used to improve the isolation between the two antenna elements. The two U-shaped slots in the ground acted as band-reject filters for the two bands of operation, where the longer loop (around a quarter-wavelength long) improved the isolation at the lower band, and the shorter

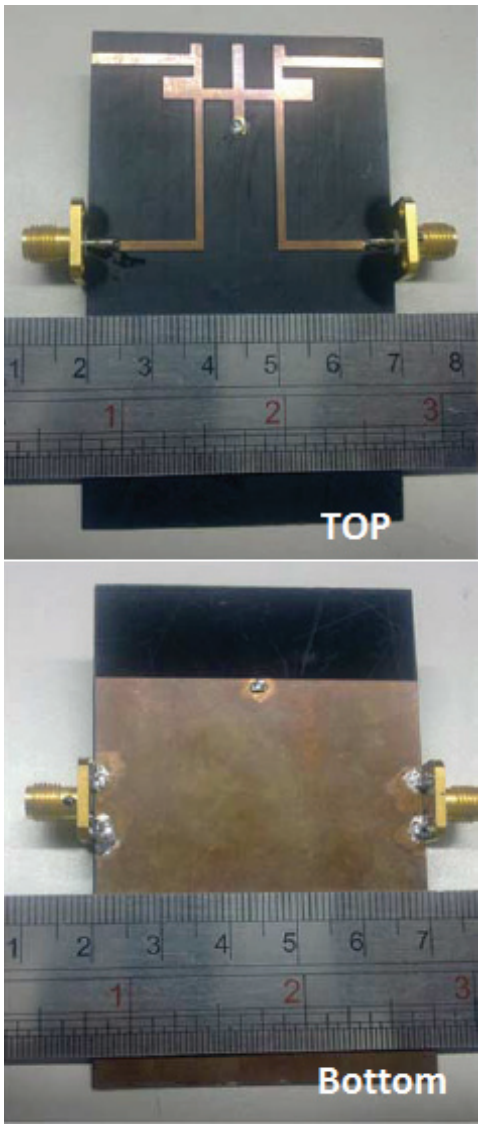

Figure 5a. The fabricated structure of a dual-band MIMO antenna system [23].

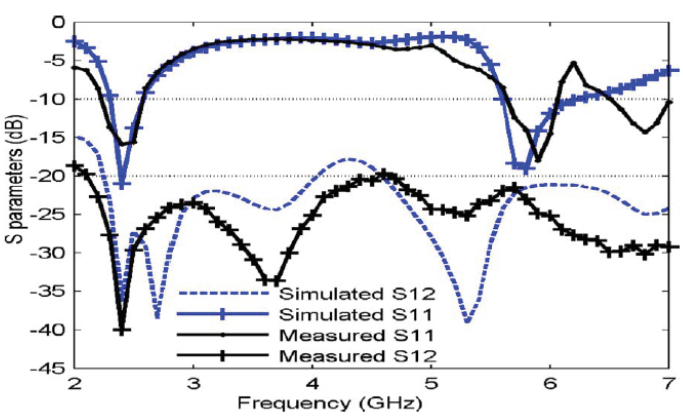

Figure 5b. The measured *S* parameters of the system in Figure 5a [23].

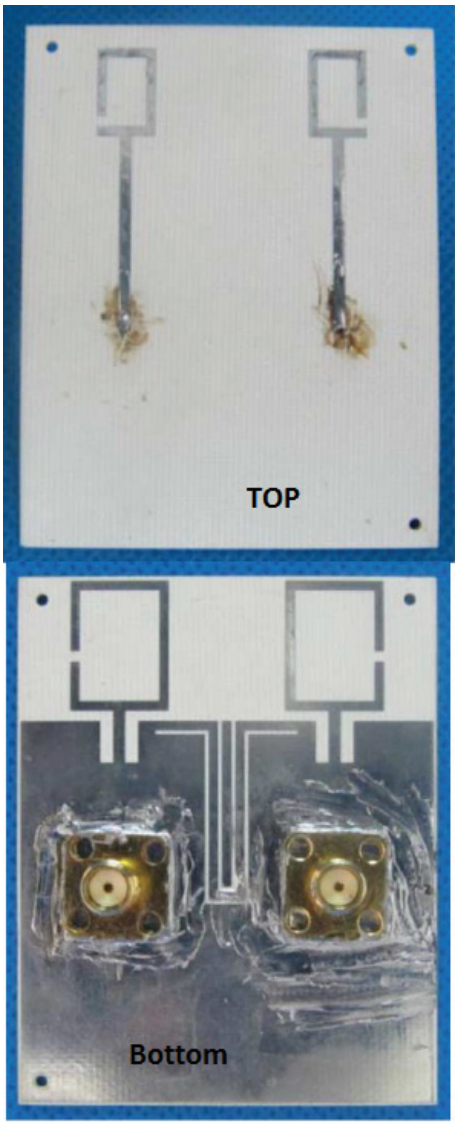

Figure 6a. The fabricated structure of a dual-band MIMO antenna system based on two open rectangular loops [29].

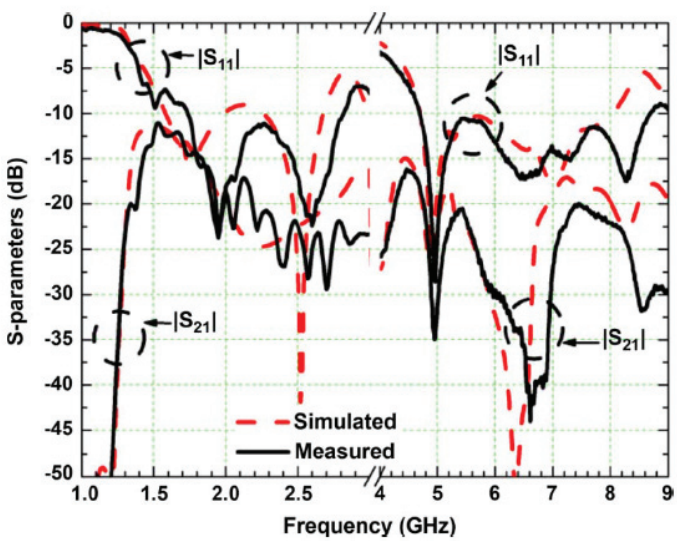

Figure 6b. The measured *S* parameters of the system in Figure 6b [29].

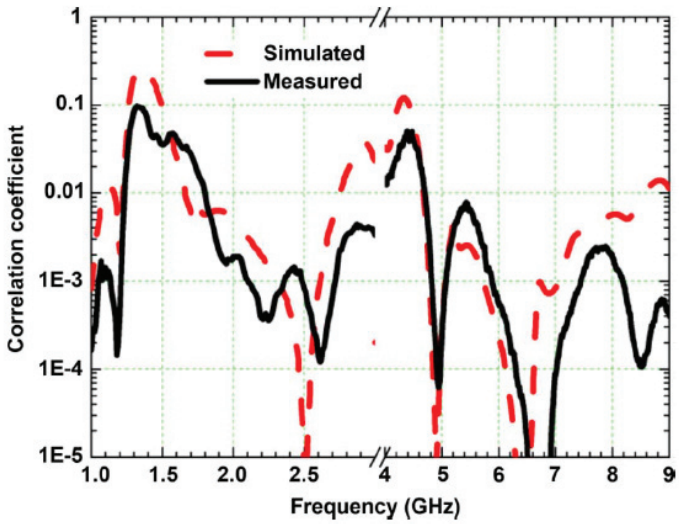

Figure 7. The correlation coefficient of the dual-band MIMO antenna system based on two open rectangular loops [29].

loop improved the higher-band isolation. A minimum efficiency of 70% was obtained across the bands of operation. A maximum correlation coefficient of 0.1 was obtained, as shown in Figure 7. The maximum measured gain was 4.5 dBi in the lower band and 7.2 dBi in the higher band. The TARC curves and mean effective gain were not evaluated in this work. The capacity loss (how much deviation from the ideal capacity that could be obtained from this MIMO configuration in the same environment) in a uniform environment and using the correlation values obtained was evaluated, and was found to be 0.3 bits/s/Hz, which was considered acceptable.

A very recent multi-band printed MIMO antenna was proposed in [32]. The antenna covered four bands, 2.28 GHz to 2.66 GHz, 3.35 GHz to 3.65 GHz, 5.07 GHz to 5.3 GHz, and 5.75 GHz to 5.85 GHz. The basic element of the printed MIMO antenna system was a combination of an open-ended and short-ended F-shaped microstrip slot. The over-all size of a single element was 33 mm × 36 mm × 1.56 mm, realized on a Rogers 4003 substrate. The isolation between the various elements in the four-element printed MIMO antenna system was more than 14 dB. This high value was due to the split in the individual ground planes of each element (no common ground plane). The efficiencies were higher than 95%. Figure 8 shows the fabricated MIMO antenna as an inset to its *S*-parameters curves.

Note that the proposed printed MIMO system had four separate ground planes on one substrate, which is not practical in a real design. However, this split would reduce the ground current, and thus would improve the isolation between the adjacent elements. Also please observe that the orientation of the antennas was made such that the pattern correlation was reduced via polarization diversity. The maximum measured gain was higher than 4 dBi in the bands of operation, with a minimum efficiency of 95%. The TARC and mean effective gain were not evaluated for this design.

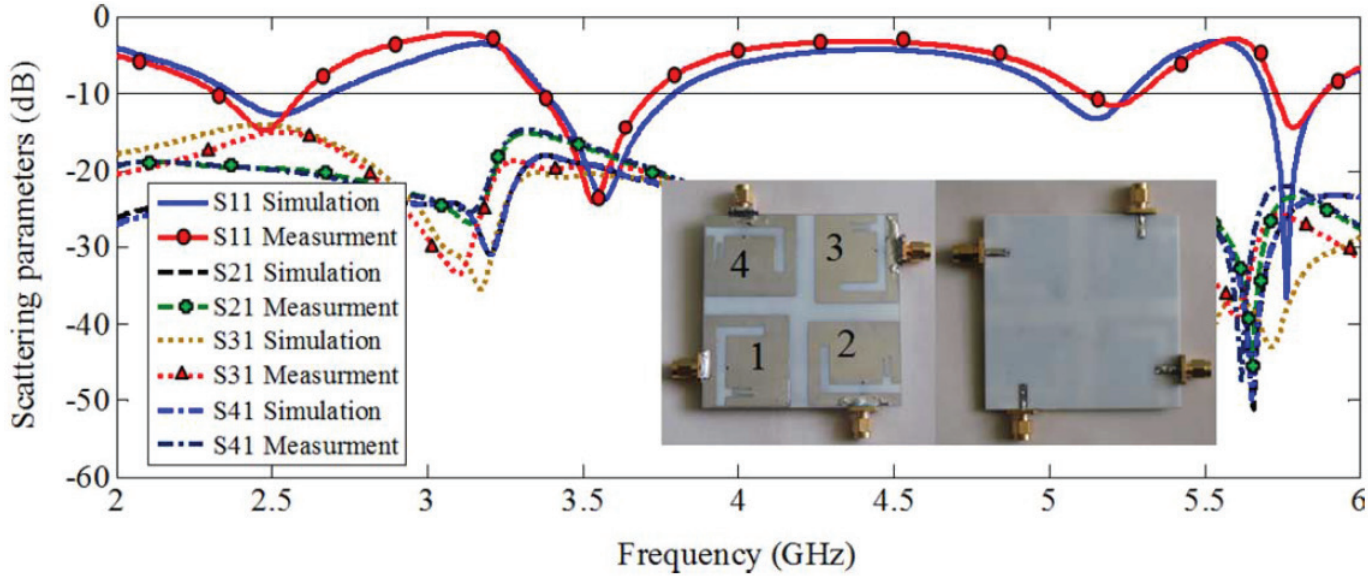

Figure 8. A four-element quad-band printed MIMO antenna system and its *S*-parameter curves [32].

3.2 Multi-Band Printed MIMO Antenna Systems with at Least One Band Operating Lower than 1 GHz

According to Figures 2 and 3, the numbers of papers and antenna designs for multi-band printed MIMO antenna systems targeting the lower bands (i.e., lower than 1 GHz) are much lower than for those targeting the higher bands, due to the difficulties in maintaining good isolation between the antenna elements when they are very close to one another in a handheld-device scenario. In this subsection, we will show some of the recent designs that provide MIMO antennas with low-band capabilities and multi-band operation. The designs in [33-41] are examples of the recent work in this domain. The interest in the lower bands has gained momentum due to the fact that 4G MIMO wireless standards started covering the 700 MHz band, and thus antennas operating at such lower bands are of interest for such standards, not to mention backward compatibility with legacy bands in the 800 MHz and 900 MHz frequencies.

In [34], a dual-element dual-band printed MIMO antenna system for 4G USB dongle applications was proposed. The antenna system covered the frequencies 0.746 GHz to 0.787 GHz and 2.5 GHz to 2.69 GHz. The antennas consisted of two printed dual-band PIFAs with a symmetric slotted strip. Isolation better than 15 dB was achieved in both bands. A shorting (neutralization) line was used to enhance the isolation. This mechanism was used to cancel out the high induced current on the victim antenna by injecting a 180° out-of-phase current from the aggressor antenna at that point, thus canceling (reducing) the current level and improving the isolation.

The efficiencies were 33% and 68% for the low and high bands, respectively. The low efficiency at the lower band was a consequence of the miniaturization of the antenna. Figure 9 shows the geometry of the proposed MIMO antenna (Figure 9a) as well as its *S*-parameter curves (Figure 9b). The correlation coefficient was less than 0.2. The total size of the FR-4 board used was 25 mm × 66 mm × 0.8 mm. The overall size of each printed element was 7 mm × 66 mm. The maximum measured gain was −0.55 dBi at 770 MHz and −0.12 dBi at 2.55 GHz. The efficiencies of the antennas were approximately 33% at the lower band and 68% at the higher band. The mean effective gain ratios were 0.93 and 1.08 in the two bands, respectively. The measured diversity gains in a reverberant chamber were 3.77 dB and 5.69 dB for the lower and higher bands, respectively. This design showed a practical USB dongle MIMO antenna system for LTE and M-WiMAX wireless standards.

The four-shaped dual-band MIMO antenna system appeared in [35] in a two-element configuration, and was presented in [36] as a four-element configuration. Figure 10 shows the diagram and the fabricated four-element four-shaped MIMO antenna system. The four-shaped antenna was a modified version of a PIFA antenna, but with a 90° bend in the main arm, and a secondary arm for dual resonance. The antenna resonated at two bands, one around 760 MHz and the other around 2.4 GHz. The bandwidth achieved in these two bands was 50 MHz and 150 MHz, respectively. Due to the close placement of the antennas in a 60 mm × 100 mm smart-phone backplane, the separation between two adjacent antennas was less than $\lambda/15$ at the lower operating band. This posed a limit on the achievable isolation.

A simple defected ground structure composed of vertical slits acting as a band-stop filter was devised in [36] to enhance the isolation between the four elements within a 58 mm × 100 mm area, while a more-complicated dual-band defected ground based on dumbbell-shaped loaded spirals was used in [34]. Significant isolation improvement was achieved using the dual-band method in [35], especially in the lower band of operation. The measured *S*-parameter curves for the four-element four-shaped MIMO antenna with vertical ground slits are shown in Figure 11. A single element occupied one-quarter of

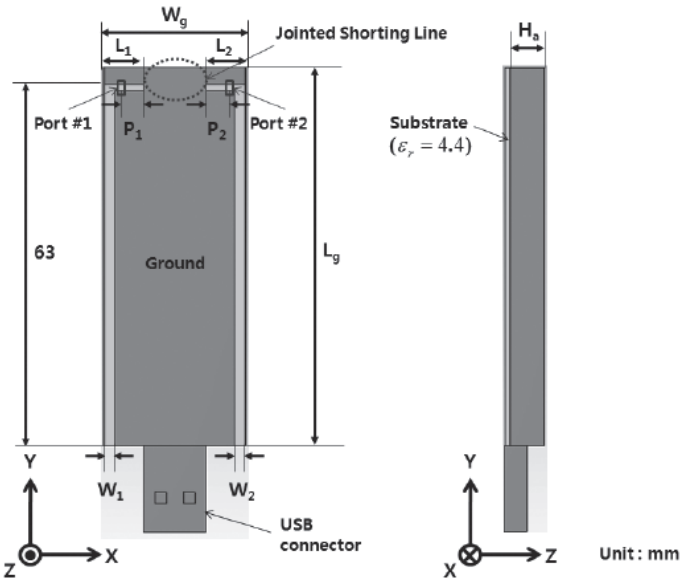

Figure 9a. A two-element dual-band printed MIMO antenna system for 4G USB dongle applications [34].

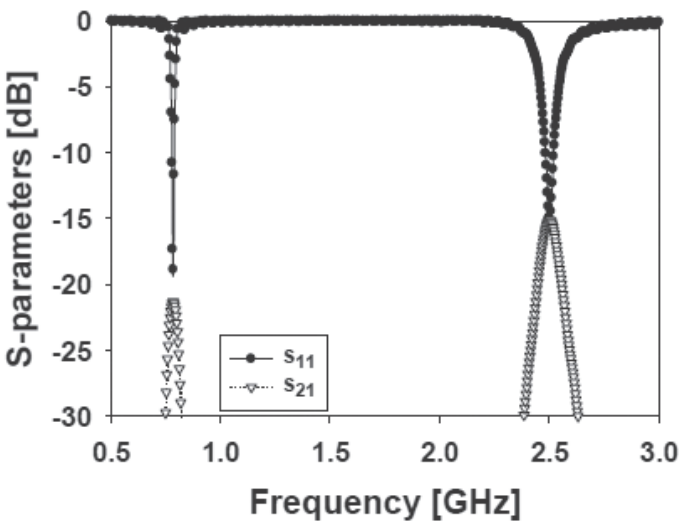

Figure 9b. The *S*-parameter curves for the system of Figure 9a [34].

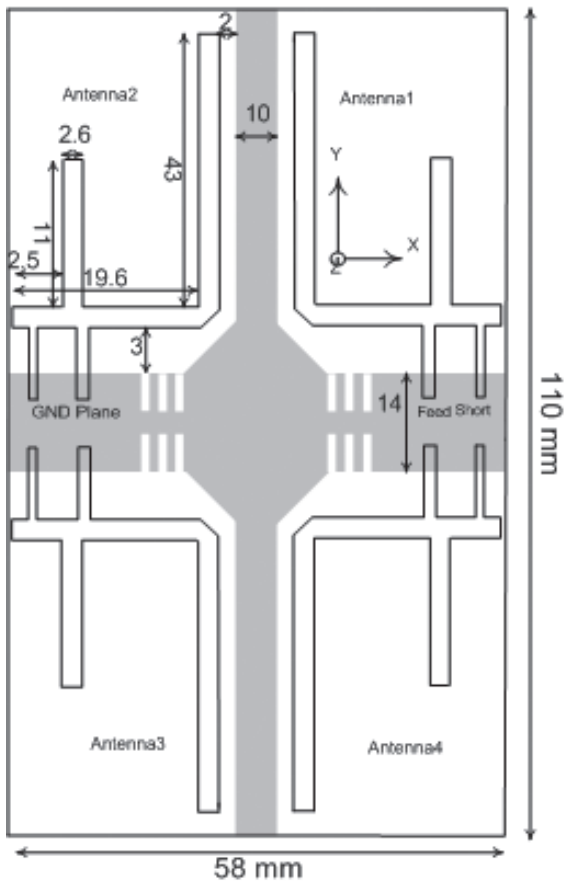

Figure 10a. The diagram of a printed four-element dual-band MIMO antenna system [36].

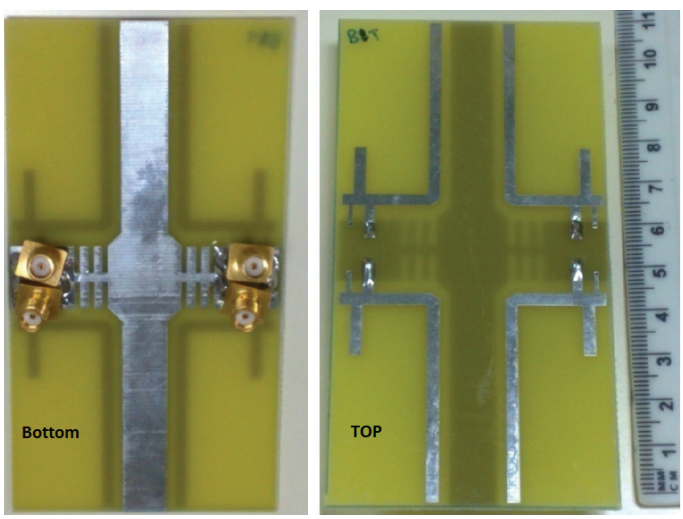

Figure 10b. The fabricated antenna for the system of Figure 10a [36].

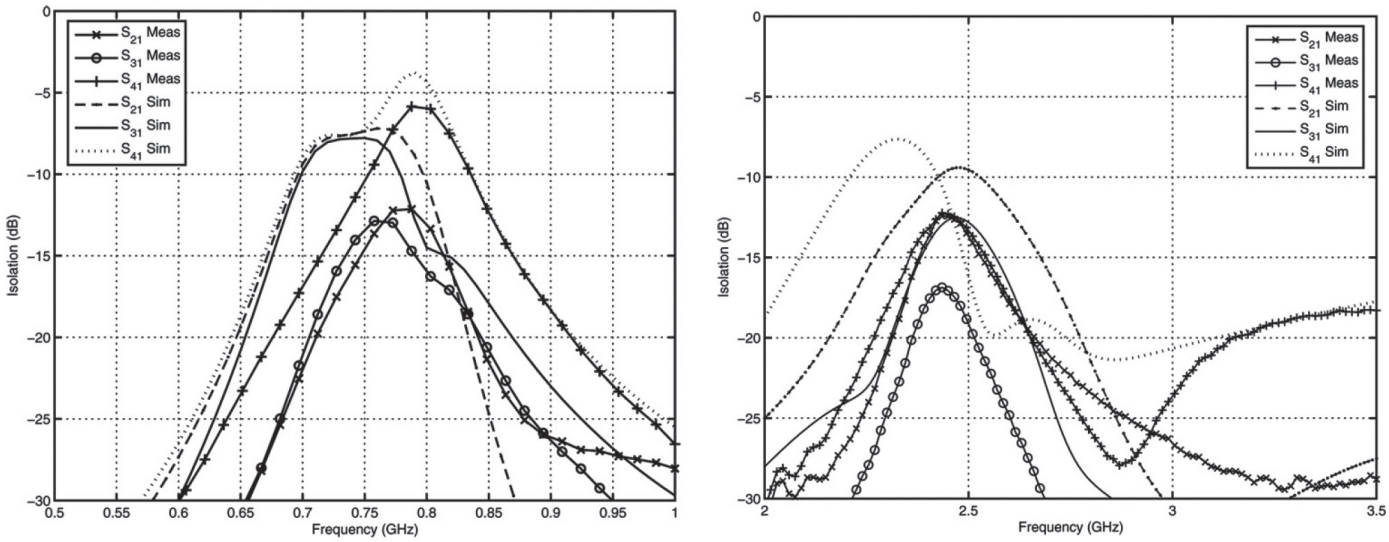

Figure 11. The measured and simulated S parameters of the four-element MIMO antenna system: (a) low band; (b) high band [36].

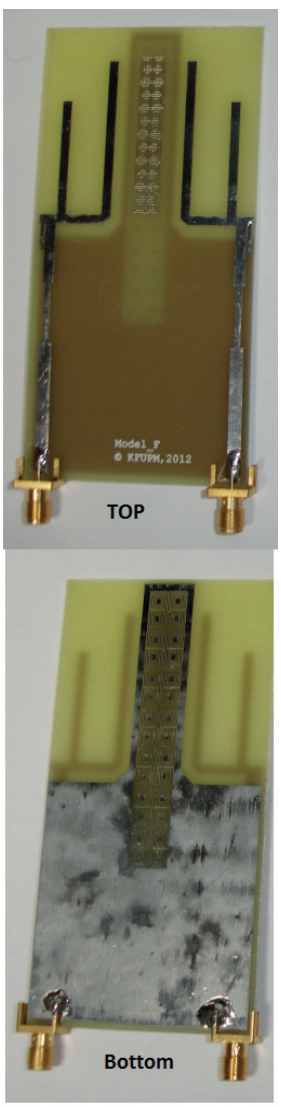

Figure 12a. A dual-element dual-band four-shaped MIMO antenna system: the fabricated antenna with MTM isolation structure [37].

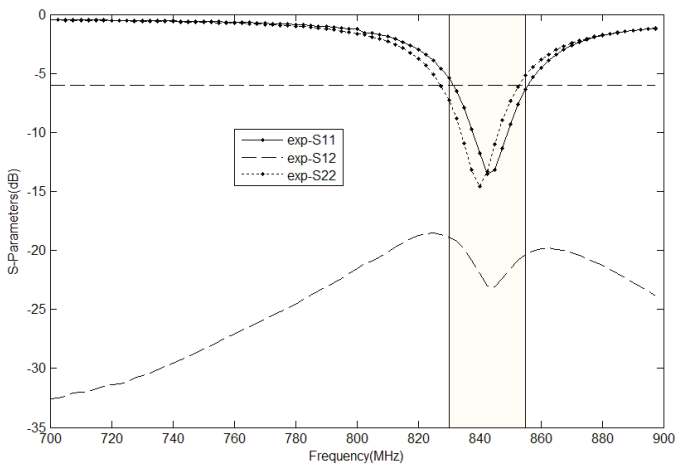

Figure 12b. The measured S parameters in the lower band for the system of Figure 12a [37].

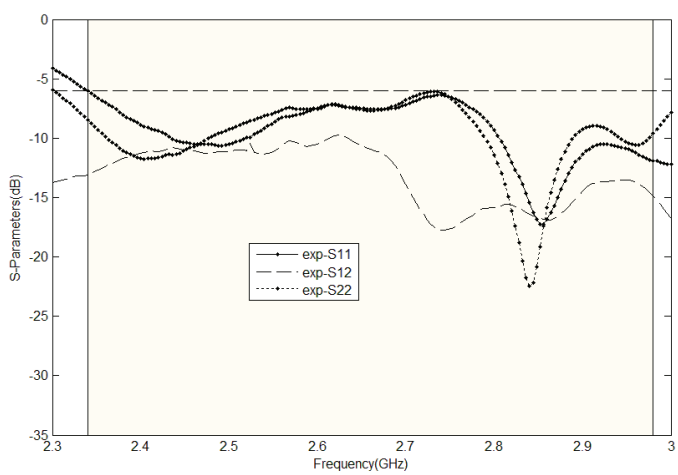

Figure 12c. The measured S parameters in the high band for the system of Figure 12a [37].

a 58 mm × 100 mm FR-4 substrate. The efficiencies in the two bands ranged between 40% to 70%, due to impedance mismatches and antenna losses. The correlation coefficients did not exceed 0.3 in all bands.

A metamaterial-based isolation-enhancement method for the four-shaped antenna was presented in [37], which improved the lower-band isolation by 10 dB and the higher-band isolation by 4 dB. The antenna structure and its measured curves are shown in Figure 12 (compare with the isolation in Figure 11). Isolation-enhancement methods for closely packed printed MIMO antenna systems are an active area of research, and several groups around the world are tackling this challenging area.

The TARC curves for the design in [37] were evaluated and are presented in Figure 13 for both bands of operation. The TARC curves for the low band were slightly affected by the phase difference between the two input ports, and thus the effective bandwidth was slightly lower than that seen from the reflection-coefficient, alone. The higher-band TARC curves were more affected by the two-antenna-element port phases, and the effective bandwidth was affected accordingly. In addition, lower isolation in the high band affected the TARC curves as well, according to Equation (6). One possible drawback of this four-shaped MIMO antenna system was that it occupied a large area of the system backplane when considered for a mobile-phone application, and thus its performance should be evaluated when it was backed with another ground plane that represented an LCD screen.

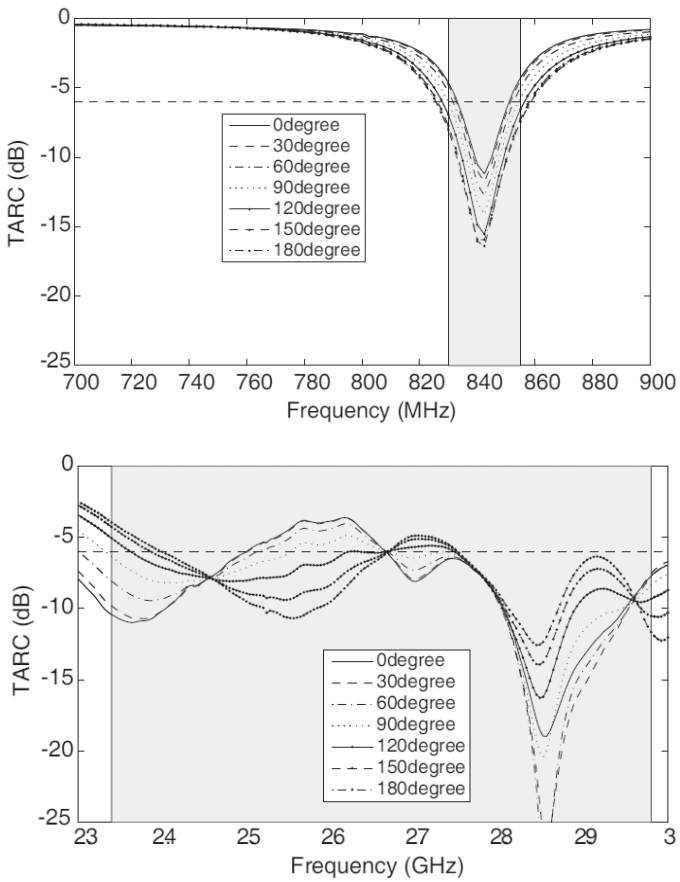

Figure 13. A dual-element dual-band four-shaped MIMO antenna system: (a) the TARC curves at the low band; (b) the TARC curves at the high band [37].

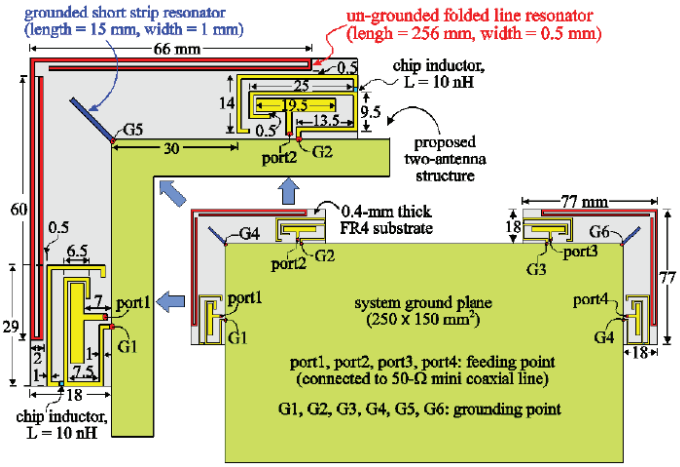

Figure 14a. The antenna structure of a tri-band four-port MIMO antenna system [41].

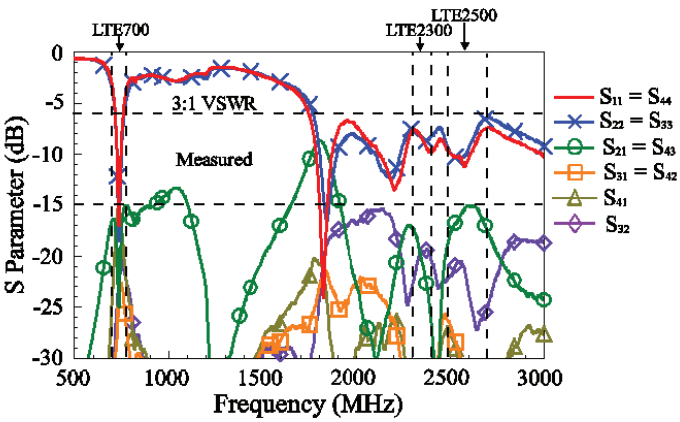

Figure 14b. The measured *S*-parameter curves for the system of Figure 14a [41].

The designs in [38-40] made use of three-dimensional raised structures to achieve the lower band of operation. It is more challenging to use only planar printed (two-dimensional) structures for the bands below 1 GHz in multi-band printed MIMO antenna systems. The work in [41] presented a tri-band printed MIMO antenna system for laptop (and large-device) applications. The antenna covered the LTE700 (704 MHz to 787 MHz), LTE2300 (2300 MHz to 2400 MHz), and LTE2500 (2500 MHz to 2690 MHz) bands. The isolation achieved over the three bands was better than 15 dB. The radiation efficiencies varied between 40% and 70%. Figure 14a shows the antenna's structure and dimensions, and Figure 14b shows the measured *S*-parameter curves.

The envelope correlation coefficient was below 0.2 over the three bands. A single antenna element occupied an L-shaped

area of 77 mm × 77 mm × 18 mm. The spatial separation between the antenna elements is a major factor for achieving good isolation for such applications due to the large size of the ground plane of the screen. The maximum measured gain was between −1 dBi to −2 dBi in the LTE700 MHz band, between 1 dBi to 3.5 dBi in the LTE2300 MHz band, and 0 dBi to 4 dBi in the LTE2500 MHz band. The efficiencies were higher than 40% in all three bands of operation. No TARC curves or mean effective gain calculations were performed for this design.

From the examples presented and the survey conducted on the area of printed multi-band MIMO antenna systems, it is clear that this area is still in need of more novel designs. These are needed to satisfy the requirements of the 4G and 5G wireless handsets by covering the lower frequency bands in the 700 MH/800 MHz bands, as well as the upper bands in the 1900 MH to 2300 MHz range, in addition to WLAN and WiMAX. Wide bandwidth is also required (at least 40 MHz) to be able to support the wider bandwidths specified in the 4G and 5G standards.

4. Conclusions

Fourth-generation wireless standards rely on MIMO technology to achieve higher data throughputs. The design of multiple printed antennas within a small-form-factor device is a challenging task. In this article, we touched upon the various metrics that are required to characterize the performance of MIMO antenna systems. We also listed several recent printed MIMO antenna system designs and examples, along with their characteristics. The area of printed MIMO antennas along with their isolation-enhancement methods is an active area of research that is of direct practical importance in consumer wireless electronics.

5.Acknowledgements

The author would like to thank the editor of the "Wireless Corner" column, as well as the reviewers, for their valuable comments, which improved the quality of the manuscript.

6. References

1. L. Song and J. Shen, *Evolved Cellular Network Planning and Optimization for UMTS and LTE*, London, CRC Press, 2011.

2. J. L. Volakis, C. C. Chen and K. Fujimoto, *Small Antennas: Miniaturization Techniques and Applications*, New York, McGraw Hill Professional, 2010.

3. R. Vaughan and J. B. Andersen, "Antenna Diversity in Mobile Communications," *IEEE Transactions on Vehicular Technology*, **36**, 4, November 1987, pp. 149-172.

4. S. Blanch, J. Romeu and I. Corbella, "Exact Representation of Antenna System Diversity Performance from Input Parameter Description," *IET Electronic Letters*, **39**, 9, May 2003, pp. 705-707.

5. P. Hallbjorner, "The Significance of Efficiencies when Using S-Parameters to Calculate the Received Signal Correlation from Two Antennas," *IEEE Antennas and Wireless Propagation Letters*, **4**, 2005, pp. 97-99.

6. 3GPP TS 36.101, V8.3.0: "EUTRA User Equipment Radio Transmission and Reception," September 2008.

7. M. A. Jensen and J. W. Wallace, "A Review of Antennas and Propagation for MIMO Wireless Communications," *IEEE Transactions on Antennas and Propagation*, **AP-52**, 11, November 2004, pp. 2810-2824.

8. E. Rajo-Iglesias, O. Quevedo-Teruel and M. Sanchez-Fernandez, "Compact MultiMode Antenna for MIMO Applications," *IEEE Antennas and Propagation Magazine*, **50**, 2, April 2008, pp. 197-205.

9. O. Quevedo-Teruel, M. Sanchez-Fernandez, M. L. Pablo-Gonzalez and E. Rajo-Iglesias, "Alternating Radiation Patterns to Overcome Angle of Arrival Uncertainty," *IEEE Antennas and Propagation Magazine*, **52**, 1, February 2010, pp. 70-79.

10.Sung Ho Chae, Se-keun Oh and Seong-Ook Park," Analysis of Mutual Coupling, Correlations, and TARC in WiBro MIMO Array Antenna," *IEEE Antenna and Wireless Propagation Letters*, **6**, 2007, pp. 122-125.

11. M. Manteghi and Y. Rahmat-Samii, "Multiport Characteristics of a Wideband Cavity Backed Annular Patch Antenna for Multipolarization Operations," *IEEE Transactions on Antennas and Propagation*, **AP-53**, 1, January 2005, pp. 466-474.

12. D. M. Pozar, *Microwave Engineering, Second Edition*, New York, John Wiley, 1998.

13. M. Manteghi and Y. R. Sami, "Broadband Characterization of the Total Active Reflection Coefficient of Multiport Antennas," IEEE Antennas and Propagation Society International Symposium (APS2003), **3**, Ohio, USA, June 2003, pp. 20-23.

14. S. Su, C. Lee and F. Chang, "Printed MIMO-Antenna System Using Neutralization-Line Technique for Wireless USB-Dongle Applications," *IEEE Transactions on Antennas and Propagation*, **AP-60**, 2, February 2012, pp. 456-463.

15. J. O. Nielsen, G. F. Pederson, K. Olesen and I. Z. Kovacs, "Computation of Mean Effective Gain from 3D Measurements," IEEE 49th Vehicular Technology Conference, **1**, Texas, USA, May 1999, pp. 787-791.

16. T. Taga, "Analysis of Mean Effective Gain of Mobile Antennas in Land Mobile Radio Environments," *IEEE Transactions on Vehicular Technology*, **39**, 2, May 1990, pp. 117-131.

17. N. Jamaly, A. Derneryd and T. Svensson, "Analysis of Antenna Pattern Overlap Matrix in Correlated Non-Uniform Multipath Environments," IEEE 7th European Conference on Antennas and Propagation (EuCAP), Gothenburg, Sweden, April 2013, pp. 2113-2117.

18. K. Kalliola, K. Sulonen, H. Laitinen, O. Kivekäs, J. Krogerus, and P. Vainikainen, "Angular Power Distribution and Mean Effective Gain of Mobile Antenna in Different Propagation Environments," *IEEE Transactions on Vehicular Technology*, **51**, 5, September 2002, pp. 823-838.

19. A. Ando, T. Taga, A. Kondo, K. Kagoshima and S. Kubota, "Mean Effective Gain of Antennas in Line-of-Sight Street Microcells with Low Base Station Antennas," *IEEE Transactions on Antennas and Propagation*, **AP-56**, 11, November 2008, pp. 3552-3565.

20. R. Vaughan and J. B. Andersen, Channels*, Propagation, and Antennas for Mobile Communications*, London, IET, 2003.

21. Z. Li, Z. Du, M. Takahashi, K. Saito and K. Ito, "Reducing Mutual Coupling of MIMO Antennas With Parasitic Elements for Mobile Terminals," *IEEE Transactions on Antennas and Propagation*, **AP-60**, 2, February 2012, pp.473-481.

22. W. Y. Li and W. J. Chen, "Concurrent 2-Port/3-Port MIMO Antenna System for UMTS/LTE 2500 Operation in the Mobile Phone," IEEE International Symposium on Antennas and Propagation (APS/URSI), Washington, USA, July 2011, pp. 1918-1921.

23. X. M. Ling and R. L. Li, "A Novel Dual-Band MIMO Antenna Array With Low Mutual Coupling for Portable Wireless Devices," *IEEE Antennas and Wireless Propagation Letters*, **10**, 2011, pp. 1039-1042.

24. J. F. Li, Q. X. Chu, and T. G. Huang "A Compact Wideband MIMO Antenna with Two Novel Bent Slits," *IEEE Transactions and Antennas and Propagation*," **AP-60**, 2, February 2012, pp. 482-489.

25. C. H. See, R. A. Abd-Alhameed, Z. Z. Abidin, N. J. McEwan and P. S. Excell, "Wideband Printed MIMO/Diversity Monopole Antenna for WiFi/WiMAX Applications," *IEEE Transactions on Antennas and Propagation*, **AP-60**, 4, April 2012, pp. 2028-2035.

26. R. Addaci, A. Diallo, C. Luxey, P. L. Thuc and R. Staraj, "Dual-Band WLAN Diversity Antenna System With High Port-to-Port Isolation," *IEEE Antennas and Wireless Propagation Letters*, **11**, 2012, pp. 244-247.

27. K. L. Wong, H. J. Jiang and Y. C. Kao, "High-Isolation 2.4/5.2/5.8 GHZ WLAN MIMO Antenna Array for Laptop Computer Application," *Microwave and Optical Technology Letters*, **55**, 2, February 2013, pp. 382-387.

28. M. Sonkki, E. A. Daviu, M. C. Fabres, M. F. Bataller and E. T. Salonen, "Improved Planar Wideband Antenna Element and Its Usage in a Mobile MIMO System," *IEEE Antennas and Wireless Propagation Letters*, **11**, 2012, pp. 826-829.

29. X. Zhou, X. Quan and R. L. Li, "A Dual-Broadband MIMO Antenna System for GSM/UMTS/LTE and WLAN Handsets," *IEEE Antennas and Wireless Propagation Letters*, **11**, 2012, pp. 551-554.

30. N. Ojaroudi and M Ojaroudi, "A Novel Design of Triple-Band Monopole Antenna For Multi-Input Multi-Output Communication," *Microwave and Optical Technology Letters*, **55**, 6, June 2013, pp. 1258-1262.

31. K. C. Lin, C. H. Wu, C. H. Lai, and T. G. Ma "Novel Dual-Band Decoupling Network for Two-Element Closely Spaced Array Using Synthesized Micro strip Lines," *IEEE Transactions on Antennas and Propagation*, **AP-60**, 11, November 2012, pp. 5118-5128.

32. R. Karimian, H. Oraizi, S. Fakhte and M. Farahani "Novel F-Shaped Quad-Band Printed Slot Antenna for WLAN and WiMAX MIMO Systems," *IEEE Antennas and Wireless Propagation Letters*, **12**, 2013, pp. 405-408.

33. B. G. Shin, M. J. Park, Y. S. Chung, B. Kim, H. Wi, B. Lee, C. W. Jung, W. Hong and J. Lee, "Diversity and MIMO Antenna for Multi-Band Mobile Handset Applications," IEEE International Symposium on Antennas and Propagation (APS/URSI), Washington, USA, July 2011, pp. 419-421.

34. M. Han and J. Choi "Dual-Band MIMO Antenna Using a Symmetric Slotted Structure for 4G USB Dongle Application," IEEE International Symposium on Antennas and Propagation (APS/URSI), Washington, USA, July 2011, pp. 2223-2226.

35. M. S. Sharawi, A. B. Numan, M. U. Khan and D. N. Aloi, "A Dual-Element Dual-Band MIMO Antenna System With Enhanced Isolation for Mobile Terminals," *IEEE Antennas and Wireless Propagation Letters*, **11**, 2012, pp. 1006-1009.

36. M. S. Sharawi, M. A. Jan and D. N. Aloi, "Four-Shaped 2 x 2 Multi-Standard Compact Multiple-Input-Multiple-Output Antenna System for Long-Term Evolution Mobile Handsets," *IET Microwaves, Antennas & Propagation*, **6**, 6, June 2012, pp. 685-696.

37. M. S. Sharawi, A. B. Numan and D. N. Aloi, "Isolation Improvement in a Dual-Band Dual-Element MIMO Antenna System Using Capacitively Loaded Loops," *Progress in Electromagnetics Research*, **134**, 2013, pp. 247-266.

38. C. Rowell and E. Y. Lam, "Multiple Frequency Band and High Isolation Mobile Device Antennas Using a Capacitive Slot," *IEEE Transactions on Antennas and Propagation*, **AP-60**, 8, August 2012, pp. 3576-3582.

39. J. F. Li and Q. X. Chu, "Tri-Band Antenna With Compact Conventional Phone Antenna And Wideband MIMO Antenna," IEEE International Symposium on Antennas and Propagation (APS/URSI), Illinois, USA, July 2012, pp. 1-2.

40. S. Zhang, K. Zhao, Z. Ying and S. He "Adaptive Quad-Element Multi-Wideband Antenna Array for User-Effective LTE MIMO Mobile Terminals," *IEEE Transactions on Antennas and Propagation*, **AP-61**, to appear, 2013, pp. 1-9.

41. W. Y. Li, W. J. Chen and C. Y. Wu, "Multiband 4-Port MIMO Antenna System for LTE700/2300/2500 Operation in the Laptop Computer," Proceedings of Asia Pacific Microwave Conference, (APMC 2012), Kaohsiung, Taiwan, December 2012, pp. 1163-1165.

Introducing the Author

Mohammad S. Sharawi is an Associate Professor of Electrical Engineering at King Fahd University of Petroleum and Minerals (KFUPM), Dhahran, Saudi Arabia. Dr. Sharawi is the founder and Director of the Antennas and Microwave Structure Design Laboratory (AMSDL). He was a Research Scientist with the Applied Electromagnetics and Wireless Laboratory in the Electrical and Computer Engineering Department, Oakland University, Michigan, USA, during 2008-2009. Dr. Sharawi was a faculty member in the Computer Engineering Department at Philadelphia University, Amman, Jordan, during 2007-2008. He served as the Organization Chair of the IEEE Conference on Systems, Signals and Devices that was held in Jordan in July 2008. He has been on several technical committees for IEEE conferences, and is a reviewer for various journals.

He obtained his PhD in RF Systems Engineering from Oakland University, Michigan, USA, in 2006. During 2002-2003, he was a hardware design engineer with Silicon Graphics Inc., California, USA. Dr. Sharawi has more than 80 refereed international journal and conference paper publications. His research interests include printed and MIMO antenna design and characterization, RF electronics, applied electromagnetics, wireless communications and hardware integration. He has one issued, three published, and seven pending patents. He is the single author of three book chapters. Dr. Sharawi is a Senior Member of the IEEE.